



REVIEW ARTICLE: FIELD TECHNIQUES

# Radiation measurement for plant ecophysiology

Hamlyn G. Jones<sup>1,4</sup>, Nicole Archer<sup>1</sup>, Eyal Rotenberg<sup>2</sup> and Raffaele Casa<sup>1,3</sup>

<sup>1</sup> Plant Research Unit, Division of Environmental and Applied Biology, School of Life Sciences, University of Dundee at SCRI, Invergowrie, Dundee DD2 5DA, UK

<sup>2</sup> Department of Environmental Sciences and Energy Research, Weizmann Institute of Science, Rehovot, 76100 Israel

<sup>3</sup> Dipartimento Produzione Vegetale, Università degli Studi della Tuscia, Via San Camillo de Lellis, 01100 Viterbo, Italy

Received 22 October 2002; Accepted 13 December 2002

## Abstract

The principles of radiation physics for plant ecophysiological studies are outlined with an emphasis on choosing appropriate sensors for specific purposes such as for studies of photosynthesis, UV-B damage or canopy energy balance. Remote sensing, both from the ground and from aircraft or satellites, is increasingly being used as a tool for the study of plant canopies. Therefore, relevant terminology and applications are discussed, including the use of remote sensing for the determination of canopy structural properties and the use of thermal remote sensing for the measurement of canopy temperature, for example, in energy balance studies.

Key words: Energy balance, infrared, irradiance, radiation, sensors, ultra-violet.

## Introduction

The aims of this review are to concentrate on aspects of radiation measurement relevant to plant environmental physiologists. For more detailed discussion of the specific basic aspects of radiation physics and fuller definitions, readers should refer to the excellent introduction by Campbell and Norman (1998). Further details may also be found in other texts (Gates, 1980; Monteith and Unsworth, 1990; Jones, 1992).

Historically, plant ecophysiologicals have largely been interested in radiant fluxes to or from vegetation, often related to total energy balance or photosynthesis, but, more recently, there has been increasing interest in the use of

remote sensing both from satellite or aircraft sensors and from ground-based sensors such as hand-held infrared thermometers. There are, however, some important differences between the approaches used in remote sensing and more conventional environmental physiology which will be developed in some detail in this review.

## Basics

### Definitions and terms

Some key definitions of quantities used for the measurement and description of radiation are summarized in Table 1.

Radiation flux/flux densities are often determined only for horizontal surfaces, even within plant canopies. For many purposes such as photosynthesis, however, it is the irradiance on the actual plane of the leaf that may be relevant. In practice, detailed measurements of the radiation distribution at the surfaces of leaves within plant canopies are rare. This is largely because of problems of replication for measurements distributed throughout canopies (Gutschick *et al.*, 1985), so estimation of the light climate for individual leaves for photosynthesis prediction is commonly based on simple models of the radiation field within canopies (see Conclusions).

*Solar/terrestrial/net radiation:* The electromagnetic spectrum is divided into a number of arbitrary wavebands depending on either the source of the photons (solar or terrestrial thermal radiation) or their interaction with living material (ultraviolet, visible, photosynthetically active, etc.). For ecophysiological purposes, the most important division is into solar radiation derived from the sun

<sup>4</sup> To whom all correspondence should be addressed. Fax: +44 (0)1382 344275. E-mail: h.g.jones@dundee.ac.uk

**Table 1.** Key definitions of terms used in description of radiation (Jones, 1992; Nicodemus et al., 1977)

Name	Units	Definition
Radiant flux	W (=J s <sup>-1</sup> )	The amount of radiant energy emitted, transmitted or received per unit time
Radiant flux density	W m <sup>-2</sup>	Radiant flux per unit area of a surface traversed by the radiation
Irradiance (or emittance)	W m <sup>-2</sup>	Radiant flux density incident on (or emitted by) a surface
Spectral irradiance (or emittance)	W m <sup>-2</sup> μm <sup>-1</sup>	The radiant flux density incident on (or emitted by) a surface per unit wavelength interval
Radiant intensity	W sr <sup>-1</sup>	Radiant flux emanating from a surface per unit solid angle
Radiance	W m <sup>-2</sup> sr <sup>-1</sup>	The radiant flux density emanating from a surface per unit solid angle
Spectral radiance	W m <sup>-2</sup> sr <sup>-1</sup> μm <sup>-1</sup>	The radiant flux density emanating from a surface per unit solid angle per unit wavelength interval
Photon flux density	μmol m <sup>-2</sup> s <sup>-1</sup>	Number of micromoles of photons emitted, transmitted or received per unit area per unit time (usually within a specified wavelength such as the photosynthetically active region (400–700 nm))
Emissivity	–	The ratio of the thermally generated radiance emitted by a body to the radiance that would be emitted by a black body (or perfect emitter) at the same temperature

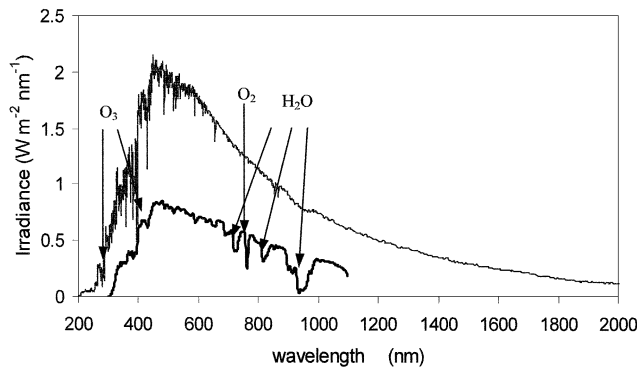


**Fig. 1.** The extraterrestrial solar spectrum (the fine line—Wehrli, 1985) and a typical solar radiation spectrum measured at the earth's surface (thick line) for 07.52 on 1 June 1987 at Cape Canaveral, Florida (Riordan *et al.*, 1990). Some atmospheric absorption bands for O<sub>3</sub>, O<sub>2</sub> and H<sub>2</sub>O are indicated.

(between about 0.3 μm and 4 μm) and terrestrial thermal radiation (4–100 μm). The energy distribution of solar radiation at the top of the Earth's atmosphere and at the Earth's surface is illustrated in Fig. 1.

**Energy/quantum processes:** Although electromagnetic radiation has wave-like properties, with an apparent wavelength, it is emitted in discrete quanta (=photons) whose energy is inversely related to wavelength ( $\lambda$ ; m) and proportional to the frequency ( $\nu$ ; s<sup>-1</sup>) of oscillation according to

$$e = hc/\lambda = h\nu \quad (1)$$

where  $e$  is the energy (J quantum<sup>-1</sup>),  $h$  is the Planck constant ( $6.63 \times 10^{-34}$  Joule s) and  $c$  is the velocity of light ( $3 \times 10^8$  m s<sup>-1</sup>). For most situations the numbers are

inconveniently small so the energy per mole of photons (or else energy per μmol photons) is more commonly used. This is obtained from  $e$  by multiplying by Avogadro's number,  $N$  ( $6.02 \times 10^{23}$  mol<sup>-1</sup>). Using these relationships one can convert the radiant energy received in any waveband into the corresponding number of quanta. For example for green light at 550 nm, 1 J is equivalent to 4.6 μmol quanta (i.e.  $(5.5 \times 10^{-7}) / (6.63 \times 10^{-34} \times 3 \times 10^8 \times 6.02 \times 10^{17})$ ) μmol quanta J<sup>-1</sup>).

**Sensors (cosine corrected/collimated/spectral irradiance):** For a parallel beam of radiation, the irradiance on a surface depends on its orientation relative to the radiant beam according to Lambert's cosine law:

$$I = I_0 \cos \theta \quad (2)$$

where  $I$  is the flux density at the surface and  $I_0$  is the flux density normal to the beam and  $\theta$  is the angle between the beam and normal to the surface. This relationship means that the irradiance on a surface decreases as the illuminating beam approaches at increasingly lower angles. It is important that radiation sensors closely approximate this ideal cosine response, otherwise they will give a biased estimate of incoming radiation on, for example, a horizontal surface, as solar angle changes.

**Reflectance (BR(D)F):** For many purposes, especially in the remote sensing of canopy properties, the interest is in the angular variation of the reflectance as the illuminating source and the detector move. A full characterization of the reflectance behaviour of a surface involves estimation of the bi-directional reflectance distribution function (BRDF), which is the ratio of the radiance reflected into an infinitesimally small solid angle at any given angle at the reflecting surface to the incident irradiance from a

given direction. When measuring radiation reflected from a surface, what is really measured is the spectral radiance (i.e. the radiant flux density emanating from a given surface per unit solid angle and per unit wavelength, expressed in  $\text{W m}^{-2} \text{sr}^{-1} \mu\text{m}^{-1}$ ). Reflectance, a ratio of incoming to outgoing radiation, can be defined in a number of ways depending on the viewing and illumination conditions: these could be directional (restricted to a small angle) or hemispherical (integrating from the whole sky or surface). Usually, in the definition of reflectance, the degree of collimation of the source followed by that of the detector are prefixed to the word reflectance (Hapke, 1993). Thus the following is known.

(a) Directional–directional (or bi-directional) reflectance, when both the illuminating and viewing angles are infinitesimally small.

(b) Directional–hemispherical reflectance, when the illuminating angle is small but the sensor view angle is so large that it integrates over the whole hemisphere above the surface.

(c) Hemispherical–directional reflectance, when the illumination comes from the whole sky and the sensor has an infinitesimally small view angle.

(d) Hemispherical–hemispherical reflectance, when the illumination comes from the whole sky and the sensor integrates over the whole hemisphere above the surface. This is also often called albedo.

Each of the above definitions can be further specified as a spectral reflectance by considering a specific wavelength, though for albedo the integrated solar spectrum broadband (0.3–4.0  $\mu\text{m}$ ) is usually employed. In reality, no sensor has an infinitesimally small view angle, nor is the sun a point source. So, strictly, the term ‘conical’ instead of ‘directional’ should be used when actual measurements are used (e.g. bi-conical reflectance), however, the term bi-directional reflectance factor (BRF) is generally used to approximate the BRDF. The BRF is defined as the ratio of the radiance reflected by a surface towards a given direction (infinitesimally small solid angle) to that which would be reflected into the same reflected-beam geometry by an ideal (lossless, i.e. having 100% reflectivity) perfectly diffuse standard surface irradiated in exactly the same way as the target surface (Nicodemus *et al.*, 1977).

### Solar radiation

The spectral irradiance at the surface of the atmosphere and an example of a spectrum at the earth’s surface are illustrated in Fig. 1. The solar constant, the wavelength integral of the extraterrestrial irradiance normal to the solar beam, is now accepted to be  $1366.1 \text{ W m}^{-2}$ . A proportion of this energy, that depends on factors such as cloudiness, atmospheric humidity and turbidity and on sun angle, is absorbed or scattered by the atmosphere. A typical solar spectrum measured at the Earth’s surface is also illustrated

and shows both the general atmospheric attenuation and the specific absorption bands due, for example, to  $\text{H}_2\text{O}$ ,  $\text{O}_2$ ,  $\text{O}_3$ , and aerosols, with  $\text{O}_3$  being particularly important in the attenuation of the shorter wave UV radiation and the total removal of the shorter ultra-violet (UV-C).

For practical purposes the solar spectrum is divided into regions with characteristic properties. The ultra-violet (UV) region describes all wavelengths less than 400 nm, and is divided into UV-A (320–400 nm), UV-B (280–320 nm) and UV-C (<280 nm). As is apparent from Fig. 1, all the UV-C, which is highly energetic and extremely damaging to DNA and life, is filtered out by  $\text{O}_2$  and  $\text{O}_3$  in the atmosphere, as is a large proportion of the UV-B. Visible solar radiation refers loosely to radiation between 400 and 700 nm. For plant ecophysiologicalists this waveband is more usefully referred to as photosynthetically active radiation (PAR), while the proportion of the solar radiation spectrum longer than 700 nm is referred to as near infrared (NIR). Approximately half the total energy in the solar spectrum is in the NIR (Monteith and Unsworth, 1990).

### Thermal radiation

All bodies emit radiation as a function of their temperature with both the energy emitted and its wavelength distribution changing with temperature according to, respectively, the Stefan–Boltzmann Law and the Planck Distribution function. The total energy emitted by a surface is a function of its temperature according to the Stefan–Boltzmann Law:

$$R_e = \epsilon \sigma T_s^4 \quad (3)$$

where  $R_e$  is the total radiant energy flux emitted per unit area ( $\text{W m}^{-2}$ ),  $\epsilon$  is the emissivity of the surface (unity for a ‘black-body’),  $\sigma$  is the Stefan–Boltzmann constant ( $=5.6703 \times 10^{-8} \text{ W m}^{-2} \text{ K}^{-4}$ ) and  $T_s$  is the surface temperature (K). The spectral distribution of the energy emitted is also a function of temperature (Wien’s Law) with  $\lambda_{\text{max}}$  increasing from 483 nm for a surface at the temperature of the sun (6000 K) to 9.65  $\mu\text{m}$  (9650 nm) for a surface at 300 K. At normal terrestrial temperatures almost all the radiation emitted falls within the range of 3–100  $\mu\text{m}$ , a wavelength region where the energy in the solar spectrum has declined to very small values (Fig. 1). This long-wave infrared is often referred to as the thermal infrared (TIR). The spectral emittance of a black-body per wavelength ( $E_{b,\lambda}$ ;  $\text{W m}^{-3}$ ) is given as a function of temperature by the Planck distribution function

$$E_{b,\lambda} = 2\pi hc^2 / (\lambda^5 [\exp(hc/k\lambda T) - 1]) \quad (4)$$

where  $k$  is the Boltzmann constant ( $1.38 \times 10^{-23} \text{ J K}^{-1}$ ). Black-bodies are perfect emitters, whose emissivity  $\epsilon=1$ , but most natural surfaces are not perfect emitters with their emissivity varying with wavelength. Nevertheless, for most practical purposes natural surfaces can be approxi-

mated as 'grey bodies' which have a constant and diffuse emissivity with no wavelength dependence.

### Purpose of measurement—implications for sensor choice

Radiation measurement is often treated too lightly by many plant physiologists and ecologists who ignore to their cost the dictum that '*the quantity (and quality) measured has to be appropriate for the purpose*'. Radiation is measured for a wide range of purposes usually relating to investigations of its potential influence on a specific ecological or physiological process such as photosynthesis, photomorphogenesis, DNA-mutagenesis or transpiration and water use. A sensor that is appropriate for one set of measurements such as a pyranometer for energy balance studies may give misleading results when used to predict photosynthetic rates in different environments.

For such studies it is not sufficient simply to 'measure the amount of light', rather it is essential to measure a quantity that relates reproducibly across a range of environments/light sources to the process under consideration. For example photosynthesis is driven by the *number of quanta* of photosynthetically active radiation *absorbed* by the photosynthetic reaction centres. Leaf energy balance and transpiration, however, are determined by the amount of *radiative energy* absorbed by the leaf. The rate of any specific physiological process is determined both by the spectral distribution of the incoming energy and by the physiological action spectrum, while in many cases where accuracy is important it is also necessary to correct incoming radiation for the absorption spectrum of the tissue of interest.

#### Action spectra

In most cases the spectral sensitivity of a sensor is only an approximation to the physiological action spectrum (i.e. the wavelength dependence of the response). Some examples of the complications that arise are illustrated in what follows.

**UV-B effects on plants:** The interest in UV-B radiation and its effects on plants have been greatly stimulated by observations on the depletion of stratospheric ozone in recent years (Farman *et al.*, 1985). Figure 2 shows the spectral response of a typical photovoltaic UV-B sensor together with some examples of plant physiological action spectra that have been reported. Combining information on the action spectrum and on the incident radiation allows the calculation of an integrated effect over the relevant wavelengths as  $\int(\text{action}_\lambda \times I_\lambda) d\lambda$ , where  $I_\lambda$  is the spectral irradiance.

To illustrate the consequences of these different responses, the relative total action for the three physio-

logical responses under either solar radiation at the top of the atmosphere or at sea level are compared in Table 2. When normalized to the UV-B sensor response, it is clear that there are rather large divergences for the different physiological responses and that the relationships between the different processes change with the incoming spectrum. In particular, the SKU430 sensor (Fig. 2) greatly underestimates DNA damage at high altitudes where there is substantial radiation with wavelengths less than 300 nm (by *c.* 3.5-fold), but overestimates it at sea level by as much as 20-fold, because in the latter case where longer wavelengths predominate, the SKU430 response is greater than the DNA-damage response curve. Similar discrepancies would be found with any broad-band sensor, and illustrate the need to select carefully the sensor used in any study, or at least to interpret any data with extreme care. In all cases the ideal would be to use a spectroradiometer and calculate the effective radiation given detailed information for the specific physiological process being studied, but cost and the conflicting requirement for adequate replication means that often this is not feasible. In situations where the spectral properties of the incoming radiation are known not to change significantly for different treatments (as in some controlled-environment studies), it is possible to use a non-matched broad-band sensor to obtain relative data on treatment differences.

A further problem that should be considered is the fact that response to UV-B is rather sensitive to the background UV-A and visible radiation which can act in a protective manner facilitating protective and repair mechanisms (Fiscus and Booker, 1995). As a result, studies of UV-B damage/sensitivity in low irradiance, controlled environ-

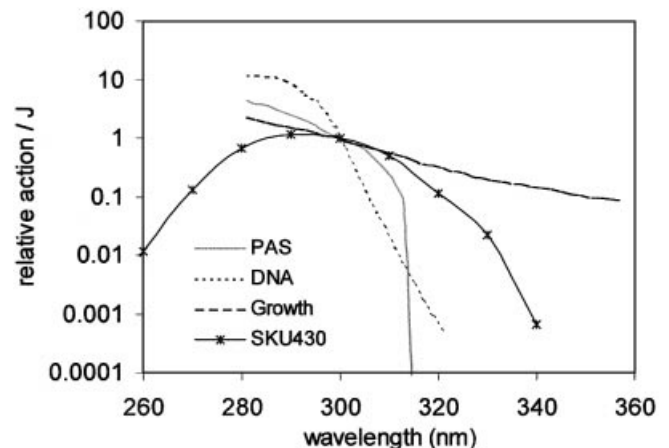


**Fig. 2.** Reported action spectra for plant physiological responses to UV-B radiation redrawn from Caldwell *et al.* (1995), where 'PAS' is Caldwell's generalized plant action spectrum, 'DNA' is Setlow's action spectrum for DNA damage in erythema, and 'growth' is Steinmuller's response for seedling growth (see Caldwell *et al.* (1995) for details). These are plotted together with the corresponding spectral response of a broad-band UV-B sensor (Skye SKU430). All response spectra are normalized to 1 at 300 nm.

**Table 2.** Integrated total action for the different action spectra shown in Fig. 2 and for solar radiation at the top of the earth's atmosphere or at sea level (from Fig. 1), calculated as  $\int(\text{action}_\lambda \times I_\lambda) d\lambda$

Values for a given radiation regime are expressed relative to the value for the SKU430 UV-B sensor. The absolute values of action (=response) for the SKU430 sensor in the two radiation regimes are shown in the final column.

	PAS	DNA	Growth	SKU	(absolute)
Above atmosphere	1.37	3.45	1.48	1.00	16.35
Sea level measurement	0.41	0.05	7.81	1.00	0.36

ments or laboratory experiments can seriously overestimate the potential effects of UV-B radiation.

**Photosynthesis and PAR:** A related problem is illustrated by photosynthesis; though the action spectrum is relatively well-defined, available sensors do not necessarily mimic that action spectrum. As a result comparisons of photosynthetic responses measured under different light sources or with different sensors from different manufacturers are difficult to compare and lead to problems of reproducibility between different laboratories. The spectral differences between a range of light sensors from one manufacturer that have been used in studies of photosynthesis are illustrated in Fig. 3; alternative sensors from other manufacturers may have different spectral responses and no specific endorsement is implied here. Although, among the sensors shown, the spectral response of the 'special PAR' sensor best mimics the photosynthetic response of plants, the 'ideal' PAR response has become the default (in spite of its deficiencies) for ensuring cross-laboratory compatibility in photosynthetic studies.

#### Conversions between light sources

Because of the different spectral properties of different light sources it is important to realize that sensors are only appropriate for conditions under which they have been calibrated. For example, although thermopile sensors generally produce an output that is proportional to energy received, whatever the source spectrum, the different spectral dependence of photovoltaic sensors means that they are less appropriate as general total short-wave energy sensors (pyranometers). Instruments such as the Skye pyranometer sensor (SKS1110) are calibrated to give correct readings in sunlight, but because they are insensitive to near infrared wavebands beyond about 1100 nm, can give serious errors if used under artificial light, and, even in the field, can seriously underestimate energy receipt underneath plant canopies outdoors.

As long as the spectral properties of the source and the sensor are known, it is possible to convert measurements in one unit (e.g. quanta in the PAR) to another unit (e.g. energy in the short wave). Approximate conversions for some common light sources may be found in Jones (1992; p.18). Unfortunately, in too many situations, data obtained

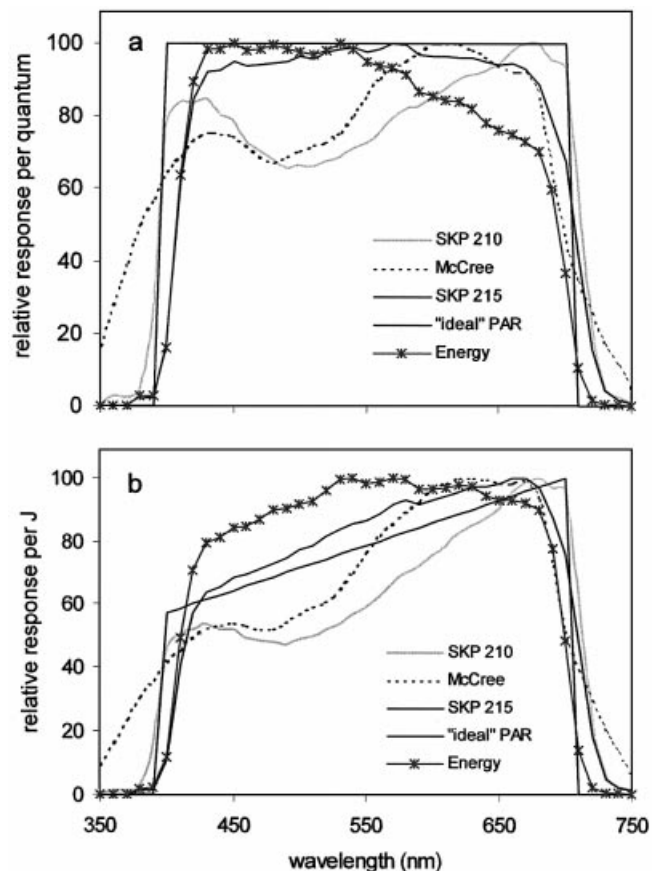


**Fig. 3.** Relative spectral responses of various radiation sensors (data kindly provided by Skye Instruments, personal communication) in comparison with an action spectrum for photosynthesis of field-grown leaves (McCree, 1972) and an 'ideal' PAR response. SKP210 is the Skye 'special PAR' sensor, tailored to the McCree photosynthetic action spectrum, SKP215 is the Skye 'ideal PAR' quantum sensor, and Energy represents the Skye SKE510 that measures energy in the PAR region. These responses are expressed (a) as response per incident quantum or (b) as response per incident Joule.

with a PAR photon sensor are used for studies where the quantity of interest is the radiant energy absorbed by canopies. Although it is possible to convert from one to the other, it is preferable to use an appropriate radiation sensor because the conversion factor is somewhat sensitive to the radiation source (e.g. time of day or position in the canopy).

## Thermal radiation measurement and applications

### Long-wave fluxes

Direct measurements of long-wave radiation fluxes have been relatively infrequent in both canopy and climatological studies, with the constituent downwelling ( $L_d$ ) and upwelling ( $L_u$ ) fluxes, or even the net flux ( $L_n$ ) being measured only rarely (Garratt, 1995; Garratt and Prata, 1996; Gilgen and Ohmura, 1999; Kessler and Jaeger, 1999). Data on the long-wave radiation fields *within* vegetation canopies are even more sparse (McGuire *et al.*, 1989; Black *et al.*, 1991; Paw U, 1992; Amthor, 1995), especially when compared with the extensive literature on short-wave radiation fields within vegetation (Ross, 1981; Myneni, 1989). The paucity of reliable data on long-wave radiation prevents adequate confirmation of the existing within vegetation long-wave radiation models (Paw U, 1992; Rotenberg *et al.*, 1998).

Long-wave radiation is difficult to measure accurately, and commonly only the net value ( $L_n$ ) is estimated as the difference between global net radiation and the net short-wave radiation. Errors in direct measurements, where they are available, may be as much as 4% (Schmetz *et al.*, 1986), which equates to at least 12–20 W m<sup>-2</sup> on typical daytime long-wave fluxes, although with best practice, modern sensors are probably capable of an accuracy of 2–3 W m<sup>-2</sup> (Philipona *et al.*, 1995, 2001; Ohmura *et al.*, 1998) on dry nights. The lack of an agreed absolute long-wave radiation reference (Field *et al.*, 1992; Halldin and Lindroth, 1992) may also be a factor. Perhaps the most important reason for the lack of data, however, is the perception that both daily and annual changes in fluxes of  $L$  are much smaller than changes in fluxes of short-wave radiation (Jones *et al.*, 2003).

### Estimation of surface temperature

In addition to the thermopile sensors commonly used for measurement of long-wave fluxes, there are a range of thermoelectric (e.g. Indium Antimonide) or microbolometer sensors that are used for remote estimation of surface temperature. The major advantage of thermal sensing of surface temperatures is that it is non-contact and rapid. The basis of the approach is the Stefan–Boltzmann Law (equation 3). Not all the radiation emitted by a surface may reach the sensor, as some wavelengths can be absorbed by atmospheric gases, and the sensors themselves are not necessarily equally sensitive to all thermal wavelengths. The types of thermal detector available make use of one of two ‘atmospheric windows’ where the air is largely transparent to thermal radiation: 3–5  $\mu\text{m}$  or 8–14  $\mu\text{m}$ . The first of these is inappropriate for outdoor measurements during the day, as these sensors may detect some reflected solar radiation; only ‘long-wave’ thermal sensors are suitable for ecophysiological studies.

Absorption by atmospheric gases can usually be ignored for measurements with short atmospheric paths (less than c. 10 m).

Estimation of surface temperature from the thermal radiant flux density involves inverting an integral of equation (3) over the relevant wavelengths, allowing for the emissivity. In practice, the approximation is usually made that the radiant flux density in the 8–14  $\mu\text{m}$  band is proportional to  $T^4$  and conversions to temperature are made in software so are invisible to the user. It is common in remote sensing applications to refer to the ‘brightness temperature’ of an object, defined as the temperature the body would need to have if it were a black-body emitting the same amount of radiation.

*Emissivity:* The emissivities of most plant leaves are between about 0.93 and 0.98, while soils are can be between about 0.60 and 0.96 (Bramson, 1968). As pointed out below, however, the effective emissivities of canopies can be significantly higher and they are often 0.98 or more.

*Background temperature:* Infrared thermography or thermometry detect the total thermal radiation flux density leaving a surface, which is the sum of the emitted thermal radiation,  $R_e$ , and the reflected thermal radiation,  $R_r$ , together with any transmitted radiation. In order to estimate the surface temperature it is necessary to measure only the emitted radiation component; this can involve estimating  $R_r$  (the transmitted component is usually assumed to be negligible in plant canopies). Different cameras have different approaches for correcting for this ‘background’ radiation. One approach is to replace the surface of interest by a highly reflective (low emissivity) diffuse reflector surface such as aluminium foil which reflects the incoming thermal radiation and then to record the apparent temperature of this surface when  $\epsilon$  is set equal to 1. This can then be used to correct the measured radiation for reflected radiation, with the correction often being incorporated within the software provided. It is worth noting that this ‘background’ temperature can vary from close to ambient air temperature when making measurements within a canopy (as the background is largely composed of other leaves at close to air temperature) to 270 K or less, compared with sensing from above when the background is dominated by the sky which may have a radiative temperature of <250 K.

Errors in estimation of emissivity ( $\epsilon$ ) can lead to significant errors in temperature estimates from the emitted radiant flux density, although the errors are smaller than one might expect from simple inversion of equation (4) which leads to the calculation that a 1% error in  $\epsilon$  should equate to a 0.75 K error in the estimated temperature at 300 K. This overestimation of the error occurs where  $\epsilon < 1$

because of the presence of reflected incoming 'background' thermal radiation so that:

$$R = (1 - \epsilon)\sigma T_{\text{background}}^4 + \epsilon\sigma T_s^4 \quad (5)$$

where  $T_{\text{background}}$  is the effective 'background' temperature. Indeed for a leaf deep within a canopy where the background temperature is close to that of the leaf itself, the apparent emissivity (i.e. the value of  $\epsilon$  required for substitution in equation (3) when the total outgoing radiation is substituted for  $R_e$ ) is close to unity, so equation (5) reduces to

$$R \cong \sigma T_s^4 \quad (6)$$

In this case, the brightness temperature is close to the actual temperature. As a fairly extreme example of the potential errors, when the background temperature is 260 K (clear sky) and the leaf temperature is 300 K, the apparent emissivity is 0.978 when  $\epsilon = 0.95$ . The firmware or software provided with thermal imagers or thermometers makes some or all of these corrections automatically, so

that temperature errors associated with errors in  $\epsilon$  are usually less than 0.3 K/% error in  $\epsilon$ .

*Radiative versus aerodynamic temperature:* For plant canopies, a major part of the energy transfer occurs through the aerodynamic processes of latent and sensible heat transfer, which depend on an effective mean canopy temperature of the surfaces involved in energy exchange. This 'aerodynamic' temperature is not necessarily identical to the radiative temperature as detected by a radiometer, which, for example, may only be seeing the upper layers of the canopy while evaporative loss may be from deeper within the canopy. This 'radiometric' temperature may differ by several degrees from the aerodynamic temperature; this complicates the estimation of canopy energy balance or evapotranspiration from radiometric temperatures, particularly because the radiometric temperature itself changes with view angle. The variation with view angle arises primarily because of varying proportions of canopy and soil within the sensor field of view as its

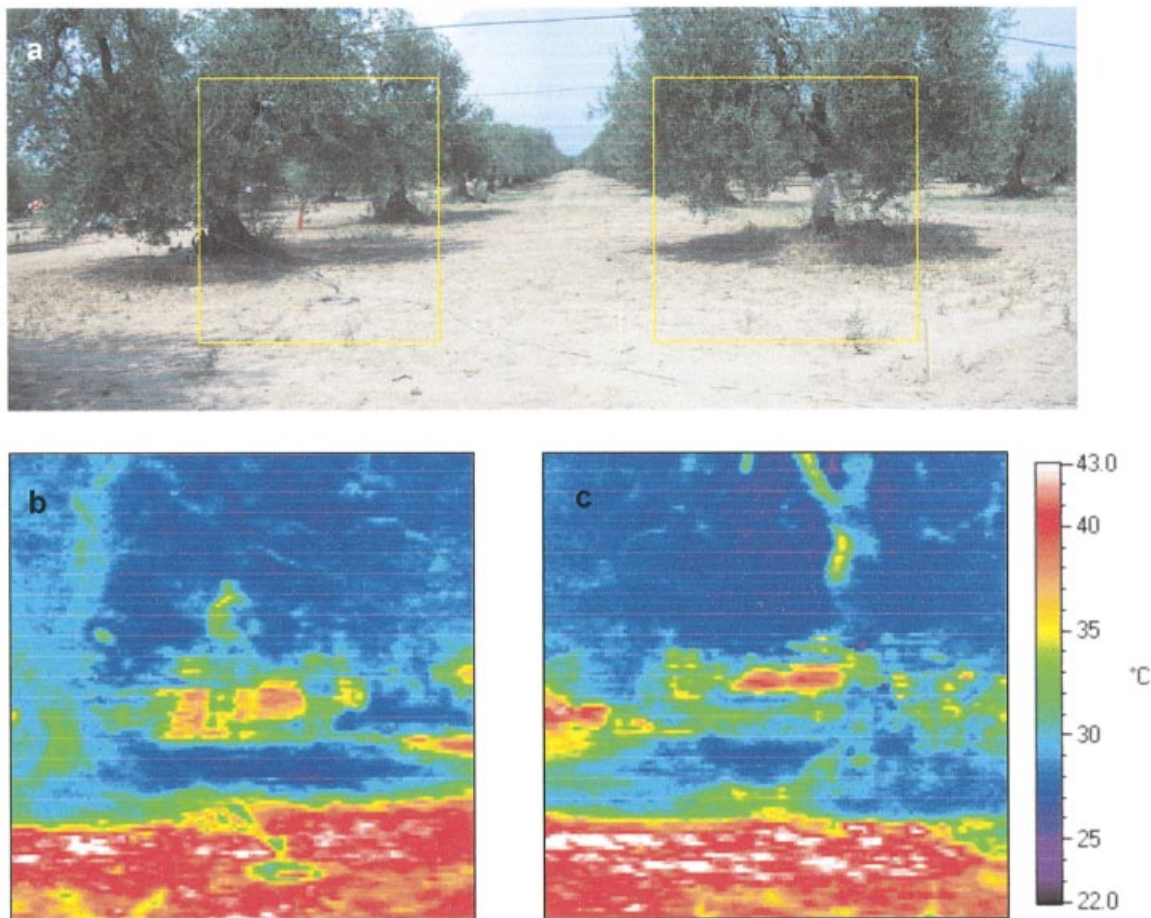


**Fig. 4.** Visible (a) and thermal images corresponding to the outlined areas (b, c) of an olive grove at Canosa di Puglia, Puglia, Italy, showing the very large range in temperatures of different canopy components on a sunny day.

zenith angle changes (at least for erect-leaved canopies there will be more of the generally hotter soil visible at nadir than at oblique views).

*Thermography in studies of canopy energy balance:* Thermography can be useful in studies of canopy energy balance, and especially for the estimation of evaporation rates (Jones *et al.*, 2003). There are, however, a number of factors that need to be considered carefully in such studies. A particular problem with spot measurements at a given moment in time arises from the differing thermal lags of different surfaces. In particular, soil temperatures react more slowly to changing radiative environments than do leaves. The time constant depends on both thermal conductivity and thermal capacity of the body itself, and the rate at which heat exchanges with the environment. Figure 4 shows comparable visible and thermal images of an olive orchard, showing the large variation in temperature of the soil and the canopy depending on factors such as exposure to the sun and water content. The short-term dynamics of the temperatures of the various components as radiation changes on a partly cloudy day are illustrated in Fig. 5. It is worth noting that the dynamics illustrated in this figure are dominated by rates of heat exchange with the atmosphere, with the soil surface temperature also having a long-term component of response depending on the soil heat flux, which itself is a function of both the thermal conductivity of the soil and its thermal capacity.

### Investigation of canopy structure

Direct measurement of canopy structure parameters is often too tedious and labour-consuming to be practically feasible and it has the additional disadvantage of being destructive or intrusive. There is, therefore, great interest in indirect methods based on radiation measurements, in particular, remote sensing methods. A range of techniques and commercially available instruments (e.g. Delta-T Sunscan, Li-cor LAI-2000, Fish-eye photography, etc.) have been developed that need the placement of sensors within or below plant canopies (Welles and Cohen, 1996). In general, these approaches are based on the measurement of either the radiation attenuation by the canopy or the gap fraction (i.e. the fraction of sky visible through the canopy at different angles). In each case it is necessary to invert a model of radiation transmission through the canopy to infer the leaf area index (LAI; leaf area/ground area) and sometimes the leaf angle distribution.

Even though instruments such as the Sunscan have 80 or more independent radiation sensors on a single probe, adequate representation of the under-canopy light climate for most heterogeneous natural canopies requires extensive replication. Nevertheless, as long as suitable replication is achieved, reasonable estimates of LAI can often be obtained, especially when the latest refinements to canopy

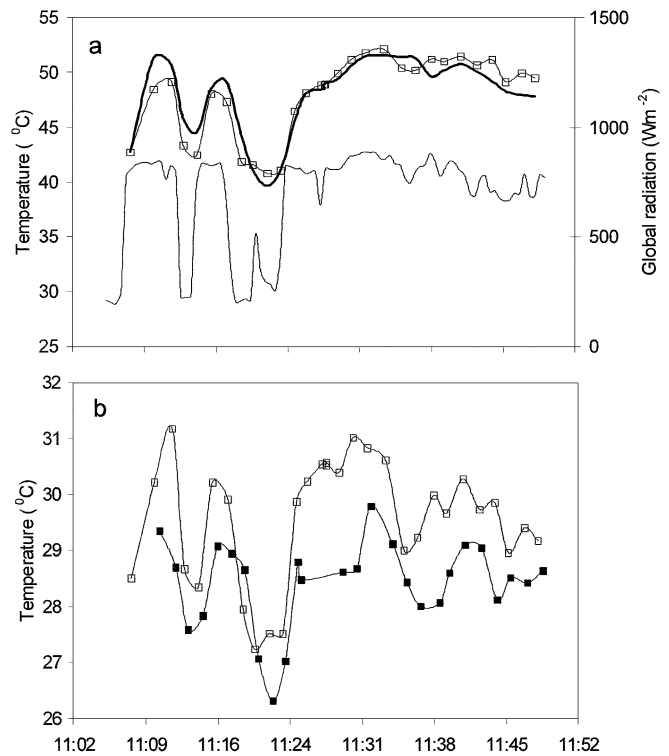


**Fig. 5.** The thermal dynamics of leaves, shaded soil and sunlit soil in an olive grove as incoming solar radiation fluctuates with passing clouds. (a) Incoming global short-wave radiation (fine line) together with the temperature of sunlit soil (open squares) and a fitted first order response curve (thick line). (b) sunlit canopy temperature (open squares) and shaded soil temperature (filled squares).

radiation transfer theory, such as those incorporating consideration of canopy gap size distribution (Chen and Cihlar, 1995) are incorporated. The major disadvantage of below-canopy measurements, however, is their limited spatial and temporal sampling, as well as sometimes their labour requirement or their restriction to specific light conditions or canopy types.

An alternative approach to within-canopy measurements is the use of above-canopy remote sensing methods which can provide a means for systematically obtaining the distribution of canopy properties over larger areas. Ground-based remote sensing has been carried out using field radiometers, often with broad band acceptance characteristics similar to those of satellite sensors. In most applications the red and NIR bands have been used, often to derive a vegetation index correlated with canopy structure parameters (Asrar *et al.*, 1984). The availability of hyperspectral field and airborne sensors and of models that incorporate simulation of leaf spectral properties into canopy BRDF models, such as the combination of models such as PROSPECT (Jacquemoud and Baret, 1990) and SAIL (Verhoef, 1984), or the Kuusk (1995) model, has stimulated a number of studies in which crop canopy properties are inferred from remote sensing by model

inversion of reflectance measurements. Using this approach it has been possible to estimate canopy characteristics including leaf area index (LAI), leaf angle distribution (LAD) and chlorophyll concentration (Jacquemoud *et al.*, 1995).

The use of multiangular remote sensing where measurements of a given target are made from several view angles, offers the possibility of exploiting the directional information, which has been shown to be especially influenced by the geometric properties of the target. Recent applications have shown the usefulness of employing directional, in addition to spectral, information for the estimation of canopy structure (Weiss *et al.*, 2000; Sandmeier *et al.*, 1999). An interesting variant on the multiangular approach to canopy analysis has been proposed by Casa and Jones (Jones and Casa, 2000; Casa and Jones, 2002) based on the observation that the fraction of shaded and sunlit leaves and soil is related to canopy structure (Hall *et al.*, 1995). Therefore, rather than assessing the reflectance, which has been the conventional approach, multiangular images are classified into the sunlit and shaded leaves and soil fractions (Casa and Jones, 2002). In principle, the variation of the proportions of each of these classes is related to both LAI and the leaf angle distribution, as shown for the example of LAI in Fig. 6. Comparison of the fractions at different view angles is

particularly useful for extracting information on the leaf angle distribution. Unfortunately, all below-canopy and above-canopy radiation measurement methods, however, become less and less accurate as LAI increases above about 4–5. Nevertheless, for many vegetation types or crop canopies, especially in dry areas, the value of LAI often does not exceed about 4.

### Conclusions: a role for modelling

Radiation interaction with vegetation is central to many of the processes of interest to ecophysiologicalists and global modellers. Although instrumentation and measurement procedures for the main fluxes are well established, there is still a need for sensors with improved spectral matching for specific physiological processes (e.g. for studies of response to UV-B) or with greater accuracy (for measurement of long-wave radiation exchanges). There is, however, an increasing recognition that there is a need for a good description of temporal and spatial variation of radiation fluxes in plant canopies if processes such as photosynthesis are to be modelled successfully (Barradas *et al.*, 1999). In many ecophysiological and productivity studies the rates of photosynthesis are now estimated on the basis of more-or-less simplified photosynthesis models which have as a required input, information on the

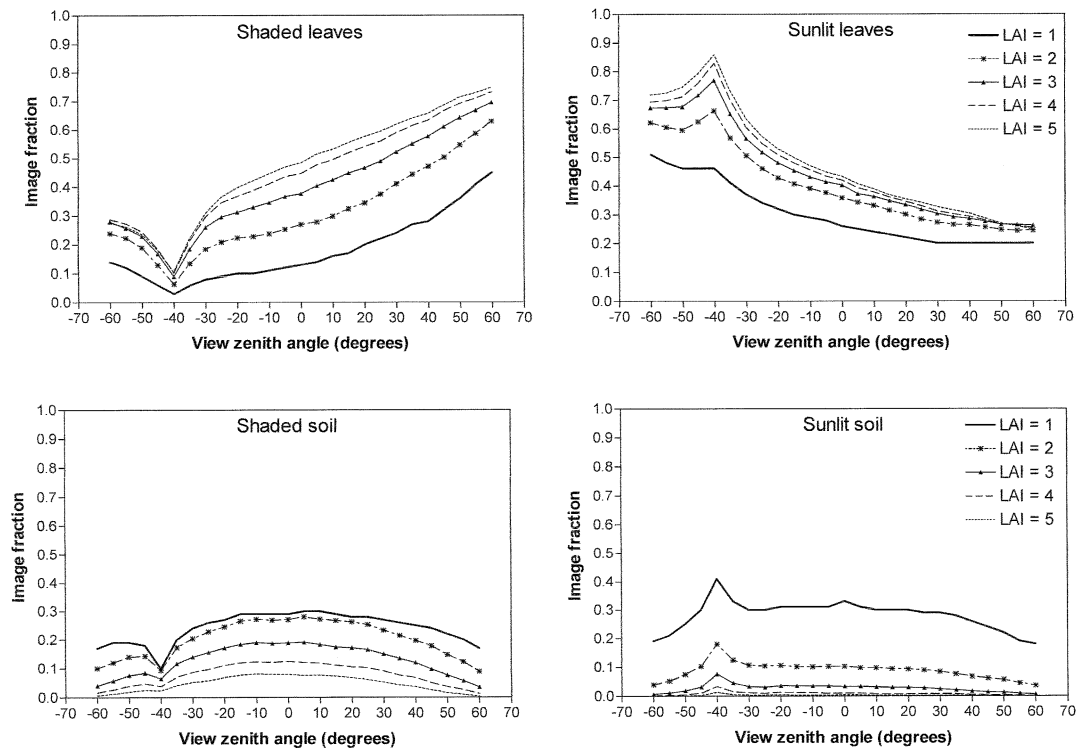


**Fig. 6.** Sensitivity of multiangular image fractions to changes in LAI. Other parameter values were:  $X=1$  (spherical leaf angle distribution), sun zenith angle= $40^\circ$ , leaf size parameter= $0.06$ ,  $FOV=6^\circ$  and camera height= $200$ . Negative view zenith angles correspond to the backscattering direction (Casa, 2002).

probability distribution of irradiance on different leaves (based on an assumed leaf angle distribution), or else incorporate a simple Beer's Law attenuation of irradiance with depth in the canopy. This modelling approach is much the most convenient, because of the great difficulty, in practice, of getting a good measure of the probability distribution function of irradiance on different leaves (Gutschick *et al.*, 1985; Barradas *et al.*, 1999). Although such probability distributions can be measured, and indeed must be measured for effective parameterization and validation of any new model, such detailed measurements are not practicable for every situation so reliance is often placed on well-trying canopy radiation models (Ross, 1981; Campbell and Norman, 1998).

Modelling is also crucial for the other developing application based on optical remote sensing for vegetation monitoring and for canopy structural analysis. Here there is a pressing need to derive simplified models of radiation interaction with vegetation which can be used with easy-to-obtain data.

## Acknowledgements

We are grateful to Belinda Trotter of Skye Instruments for data on spectral responses of Skye radiation sensors, and to the European Commission (contract EVKI-2000-22061) for funding.

## References

- Amthor JS.** 1995. Predicting effects of atmospheric CO<sub>2</sub> partial pressure on forest photosynthesis. *Journal of Biogeography* **22**, 269–280.
- Asrar G, Fuchs M, Kanemasu ET, Hatfield JL.** 1984. Estimating absorbed photosynthetic radiation and leaf-area index from spectral reflectance in wheat. *Agronomy Journal* **76**, 300–306.
- Barradas VL, Jones HG, Clark JA.** 1999. Leaf orientation and distribution in a *Phaseolus vulgaris* L. crop and their relation to light microclimate. *International Journal of Biometeorology* **43**, 64–70.
- Black TA, Chen JM, Lee XH, Sagar RM.** 1991. Characteristics of shortwave and longwave irradiances under a Douglas-fir forest stand. *Canadian Journal of Forest Research* **21**, 1020–1028.
- Bramson MA.** 1968. *Infrared radiation*. New York: Plenum Press.
- Caldwell MM, Teramura AH, Tevini M, Bornman J, Björn LO, Kulandaivelu G.** 1995. Effects of increased solar ultraviolet radiation on terrestrial plants. *Ambio* **24**, 166–173.
- Campbell GS, Norman JM.** 1998. *An introduction to environmental biophysics*, 2nd edn. New York: Springer.
- Casa R.** 2002. Multiangular remote sensing of crop canopy structure for plant stress monitoring. PhD thesis, University of Dundee.
- Casa R, Jones HG.** 2002. Retrieval of crop canopy properties: a comparison between model inversion from hyperspectral data and image classification. Proceedings NERC meeting 'Field spectral measurements in remote sensing', Southampton, UK, 15–16.
- Chen JM, Cihlar J.** 1995. Plant canopy gap size analysis theory for improving optical measurements of leaf area index. *Applied Optics* **34**, 6211–6222.
- Farman JC, Gardiner BG, Shanklin JD.** 1985. Large losses of total ozone in Antarctica reveal seasonal ClO<sub>x</sub>-NO<sub>x</sub> interaction. *Nature* **315**, 207–210.
- Field RT, Fritschen LJ, Kanemasu ET, Smith EA, Stewart JB, Verma SB, Kustas WP.** 1992. Calibration, comparison, and correction of net-radiation instruments used during life. *Journal of Geophysical Research, Atmospheres* **97**, 18681–18695.
- Fiscus EL, Booker FL.** 1995. Is increased UV-B a threat to crop photosynthesis and productivity? *Photosynthesis Research* **43**, 81–92.
- Garratt JR.** 1995. Observed screen (air) and GCM surface screen temperatures—implications for outgoing longwave fluxes at the surface. *Journal of Climate* **8**, 1360–1368.
- Garratt JR, Prata AJ.** 1996. Downwelling longwave fluxes at continental surfaces—a comparison of observations with GCM simulations and implications for the global land surface radiation budget. *Journal of Climate* **9**, 646–655.
- Gates DM.** 1980. *Biophysical ecology*. New York: Springer-Verlag.
- Gilgen H, Ohmura A.** 1999. The global energy balance archive. *Bulletin of the American Meteorological Society* **80**, 831–850.
- Gutschick VP, Barron MH, Waechter DA, Wolf MA.** 1985. Portable monitor for solar radiation that accumulates irradiance histograms for 32 leaf-mounted sensors. *Agricultural and Forest Meteorology* **33**, 281–290.
- Hall FG, Shimabukuro YE, Huemmrich KF.** 1995. Remote sensing of forest biophysical structure using mixture decomposition and geometric reflectance models. *Ecological Applications* **5**, 993–1013.
- Haldin S, Lindroth A.** 1992. Errors in net radiometry—comparison and evaluation of 6 radiometer designs. *Journal of Atmospheric Oceanic Technology* **9**, 762–783.
- Hapke B.** 1993. *Theory of reflectance and emittance spectroscopy*. Cambridge University Press.
- Jacquemoud S, Baret F.** 1990. PROSPECT—a model of leaf optical-properties spectra. *Remote Sensing of Environment* **34**, 75–91.
- Jacquemoud S, Baret F, Andrieu B, Danson FM, Jaggard K.** 1995. Extraction of vegetation biophysical parameters by inversion of the PROSPECT+SAIL models on sugar beet canopy reflectance data. Application to TM and AVIRIS sensors. *Remote Sensing of Environment* **52**, 163–172.
- Jones HG.** 1992. *Plants and microclimate*, 2nd edn. Cambridge: Cambridge University Press.
- Jones HG, Casa R.** 2000. The use of the VIFIS (Variable Interference Filter Imaging Spectrometer) to obtain information on vegetation properties using multiangular data. *Remote Sensing Reviews* **19**, 133–144.
- Jones HG, Archer NA, Rotenberg E.** 2003. Thermal radiation, canopy temperature and evaporation from forest canopies. In: Mencuccini M, ed. *Forests at the earth atmosphere interface*. Farnham Royal: Commonwealth Agricultural Bureaux (in press).
- Kessler A, Jaeger L.** 1999. Long-term changes in net radiation and its components above a pine forest and a grass surface in Germany. *International Journal of Climatology* **19**, 211–226.
- Kuusik A.** 1995. A fast, invertible canopy reflectance model. *Remote Sensing of Environment* **51**, 342–350.
- McGuire MJ, Balick LK, Smith JA, Hutchison BA.** 1989. Modelling directional thermal radiance from a forest canopy. *Remote Sensing of Environment* **27**, 169–186.
- McCree KJ.** 1972. The action spectrum, absorptance and quantum yield of photosynthesis in crop plants. *Agricultural Meteorology* **9**, 191–216.
- Monteith JL, Unsworth MH.** 1990. *Principles of environmental physics*, 2nd edn. London: Edward Arnold.
- Myneni RB.** 1989. A review on the theory of photon transport

- in leaf canopies. *Agricultural and Forest Meteorology* **45**, 1–153.
- Nicodemus FF, Richmond JC, Hsia JJ, Ginsberg IW, Limperis TL.** 1977. *Geometrical considerations and nomenclature for reflectance*. National Bureau of Standards Monograph. US Government Printing Office.
- Paw U KT.** 1992. Development of models for thermal infrared radiation above and within plant canopies. *Isprs Journal of Photogrammetry and Remote Sensing* **47**, 189–203.
- Philipona R, Frohlich C, Betz C.** 1995. Characterization of pyrgeometers and the accuracy of atmospheric long-wave-radiation measurements. *Applied Optics* **34**, 1598–1605.
- Philipona R, Dutton EG, et al.** 2001. Atmospheric longwave irradiance uncertainty: pyrgeometers compared to an absolute sky-scanning radiometer, atmospheric emitted radiance interferometer, and radiative transfer model calculations. *Journal of Geophysical Research-Atmospheres* **106(D22)**, 28129–28141.
- Ohmura A, Dutton EG, Forgan B, et al.** 1998. The baseline surface radiation network (BSRN/WCRP): new precision radiometry for climate research. *Bulletin of the American Meteorological Society* **79**, 2115–2136.
- Riordan CJ, Myers DR, Hulstrom RL.** 1990. *Spectral radiation database documentation*, Vols I, II. Golden, Colorado: Solar Energy Research Institute. ([http://rredc.nrel.gov/solar/pubs/spectral/Vol\\_2/fsec/list.html](http://rredc.nrel.gov/solar/pubs/spectral/Vol_2/fsec/list.html) jun87)
- Ross J.** 1981. *The radiation regime and architecture of plant stands*. The Hague: Dr W Junk.
- Rotenberg E, Mamane Y, Joseph JH.** 1998. Long wave radiation regime in vegetation–parameterizations for climate research. *Environmental Modelling Software* **13**, 361–371.
- Schmetz P, Schmetz J, Raschke E.** 1986. Estimation of daytime downward longwave radiation at the surface from satellite and grid point data. *Theoretical and Applied Climatology* **37**, 136–149.
- Sandmeier SR, Middleton EM, Deering DW, Qin WH.** 1999. The potential of hyperspectral bidirectional reflectance distribution function data for grass canopy characterization. *Journal of Geophysical Research-Atmospheres* **104**, 9547–9560.
- Verhoef W.** 1984. Light scattering by leaf layers with application to canopy reflectance modeling: the SAIL model. *Remote Sensing of Environment* **16**, 125–141.
- Wehrli C.** 1985. *Extraterrestrial solar spectrum*. Publication no. 615. Davos Dorf, Switzerland: Physikalisch-Meteorologisches Observatorium and World Radiation Center (PMO/WRC), July 1985.
- Welles JM, Cohen S.** 1996. Canopy structure measurement by gap fraction analysis using commercial instrumentation. *Journal of Experimental Botany* **47**, 1335–1342.
- Weiss M, Baret F, Myneni RB, Pragnère A, Knyazikhin Y.** 2000. Investigation of a model inversion technique to estimate canopy biophysical variables from spectral and directional reflectance data. *Agronomie* **20**, 3–22.